Temperature-Dependent Optical Properties of Zn and Cd: A Theoretical Study

R. V. KASOWSKI*
Department of Physics and James Franck Institute, The University of Chicago Chicago, Illinois 60637
(Received 7 April 1969)

The optical properties of Zn and Cd are investigated theoretically at $T=0°K$; a nonlocal empirical pseudopotential determined from Fermi-surface measurements is used to calculate the optical spectra at $T=0°K$. To study the temperature dependence of the spectra, we modified the $T=0°K$ pseudopotential to include lattice vibrations and thermal expansion, and then calculated the optical spectra of Cd at $T=462°K$. Fairly good agreement with experiment in regard to line shape is found if these temperature effects are properly taken into account; however, the absolute magnitudes of the calculated optical spectra exceed the experimental values by about a factor of 2.

I. INTRODUCTION

THE pseudopotential formalism[1] has been widely applied in the study of many crystals. These pseudopotentials (PP) have been determined by two different methods: (1) first-principles calculations and (2) empirical determinations from experimental data. Both methods have proved fruitful in furthering our understanding of the electronic properties of many crystals.

The hexagonal-close-packed (hcp) polyvalent metals Zn and Cd satisfy ideally the necessary conditions for the successful application of the PP formulation. Both are simple metals and have filled s, p, and d core states which provide a good basis set for orthogonalization of the plane-wave states.

Stark and Falicov[2] (SF) have calculated an empirical nonlocal PP for Zn and Cd by adjusting a set of PP coefficients to agree with the de Haas–van Alphen (dHvA) frequencies of each. The PP for Cd has already been quite successful on three different fronts: (1) The Fermi surface for this PP shows excellent agreement with detailed radio-frequency size effect measurements[3]; (2) the phonon mass enhancement predicted by this model agrees with that extracted from superconductivity experiments[4]; and (3) the trend of the experimentally measured temperature dependence of the Knight shift is explained.[5] In fact, this PP should be quite successful in predicting for Cd any transport phenomena which depend on the electronic states at the Fermi surface.[6] The PP for Zn should prove equally successful. Thus far, it has only been used to calculate the phonon mass enhancement, which, as in Cd, is found to be in close agreement with the value extracted from superconductivity data.

The use of Fermi-surface data to fit the PP parameters is not a novel approach for determining band structures and has been previously applied to many metals, e.g., Na [7] and Al.[8] In both these simple metals, the one-electron PP theory of band structures gives a good account of the energy levels near the Fermi surface. It was thus assumed that the PP also could predict correctly the one-electron states away from the Fermi surface. An excellent test of this hypothesis is to calculate the optical properties; the optical absorption $\epsilon_2(\omega)$ (in the random-phase approximation) depends directly on single-electron excitations from states below the Fermi energy to states above it.

The location and shape of the resulting interband absorption for Al [8] and Na [7] agreed with experiment, but the magnitude of the observed interband absorption exceeded the theoretically predicted value by a factor of about 2. Agreement in location and shape of the interband spectra indicates that the energy levels within 2 eV of the Fermi surface are correctly given by the PP (from Fermi-surface data), as was initially assumed. However, the exact source of the discrepancy in magnitude is still not settled, but it is thought that the calculated interband oscillator strengths are too small[9]; thus the one-electron approximation for calculating interband oscillator strengths may not be valid in metals (although quite satisfactory results are obtained for insulators and semiconductors).

Fermi-surface data have also been used to calculate an empirical one-electron potential for Cu.[10] The calculation is a good deal more complicated, since Cu is not a simple metal and d bands are actually involved. However, the important point is that the agreement between the experimental and theoretical calculation[10] of $\epsilon_2(\omega)$ produces reasonable line shapes for $\hbar\omega \geq 4$ eV; but the calculated peak at 4 eV is almost twice as large

* National Science Foundation Predoctoral Fellow.

[1] A full discussion of the pseudopotential formalism, including references to its first contributors, can be found in W. A. Harrison, *Pseudopotentials in the Theory of Metals* (W. A. Benjamin, Inc., New York, 1966).

[2] R. W. Stark and L. M. Falicov, Phys. Rev. Letters **19**, 795 (1967); and (to be published).

[3] R. C. Jones, R. G. Goodrich, and L. M. Falicov, Phys. Rev. **174**, 672 (1968).

[4] P. B. Allen, M. L. Cohen, L. M. Falicov, and R. V. Kasowski, Phys. Rev. Letters **21**, 1794 (1968).

[5] R. V. Kasowski (to be published).

[6] R. A. Young, J. Ruvalds, and L. M. Falicov, Phys. Rev. **178**, 1043 (1969).

[7] J. A. Appelbaum, Phys. Rev. **144**, 435 (1966).

[8] H. Ehrenreich, H. Philipp, and B. Segall, Phys. Rev. **132**, 1918 (1963).

[9] J. C. Phillips, in *Optical Properties and Electronic Structure of Metals and Alloys*, edited by F. Abeles (North-Holland Publishing Co., Amsterdam, 1966).

[10] F. M. Mueller and J. C. Phillips, Phys. Rev. **157**, 600 (1967).

in magnitude as that obtained experimentally. This is just the opposite to the results for the simple metals Na and Al.

The purpose of this paper is twofold: (1) to calculate the optical properties of Zn and Cd and thereby test once again (as was done for Na and Al) whether a PP,[2] determined solely from Fermi-surface properties, correctly predicts the valence and conduction-band states throughout the Brillouin zone, and (2) under the assumption that the PP is correct, to test whether the calculation of the oscillator strengths in the single-particle nearly-free-electron direct-transition model is valid in Cd and Zn, whereas it is suspected not to be valid in Al and Na.

We should add that this test involves the study of strongly nonlocal PP's (they are mostly d-like in character for Zn and Cd) in contraposition to the previous cases, where the PP is local.

Little experimental work has been done on the optical properties of Zn and Cd. Two independent experiments have been performed on Zn,[11,12] and only one for Cd.[12] All of these experiments were done by using a modified Drude reflection technique whereby plane-polarized monochromatic light is incident on a polished metal surface at an oblique angle. The measurements were performed on single crystals that had been exposed to air. Further experimental measurements which minimize the effects of oxide layers (i.e., normal incidence reflectance) would be useful for comparison with the calculated spectra and previous experiments.

The reported optical data on Zn and Cd show quite surprising behavior in two respects:

(1) The magnitudes of the absorption peaks have a large temperature dependence. The peaks at $T=298°\mathrm{K}$ exceed those at $T=77°\mathrm{K}$ by as much as 50%.

(2) The differences in optical spectra between Zn and Cd are quite large considering the otherwise strong similarities in electronic properties (dHvA frequencies, mass enhancement) and c/a ratio.

Thus, in advance, we might expect poor agreement between the calculated optical properties at $T=0°\mathrm{K}$ and the experimental spectra for $T=77°\mathrm{K}$ and $T=298°\mathrm{K}$. Furthermore, the band structures of Cd and Zn are quite similar at $T=0°\mathrm{K}$, and therefore optical spectra calculated with these band structures will be quite similar with respect to shape and magnitude.

The temperature dependence of the Knight shift in Cd[13] (which is about eight times that of any other metal in the temperature range from 0°K to melting) has been explained[14] by incorporating temperature effects (thermal lattice vibrations and thermal expansion) into the $T=0°\mathrm{K}$ PP of SF. The effect of temperature is to reduce the matrix elements of the PP by e^{-W}, where e^{-2W} is the Debye-Waller factor. We find that this temperature-dependent PP enables us to explain qualitatively the optical line shape of Zn and Cd as well as the position of the absorption peaks. The discrepancy in magnitudes between experiment and theory cannot be fully accounted for. Further experimental work is in any case highly desirable.

A dielectric formalism is discussed in Sec. II. Section III contains a discussion of the band structures and their temperature dependence. Section IV gives the details of the computational procedure, and Sec. V contains the calculated optical spectra and their comparison to experiment.

II. DIELECTRIC FORMALISM

As stated previously, the purpose of this paper is to investigate the single-particle PP of SF several eV away from the Fermi surface by studying the optical-absorption spectrum. The two major contributions to this spectrum are (1) intraband Drude currents and (2) interband currents. Only the interband current is of interest here; this contribution to the dielectric response of the crystal can be computed in the random-phase approximation by assuming that only direct interband transitions, in which the photon $\mathbf{k}$ vector is ignored in comparison to the electron $\mathbf{k}$ vector, contribute to $\epsilon_2(\omega)$. The resulting expression[15] for the imaginary part of the diagonal component jj of the dielectric tensor $\epsilon(\omega)$ is

$$\epsilon_2{}^{jj}(\omega)=\frac{4\pi^2e^2\hbar^2}{m^2\omega^2}\sum_{sn}\int\frac{1}{(2\pi)^3}\times\delta(E_{ns}(\mathbf{k})-\hbar\omega)\,|M_{ns}{}^{j}(\mathbf{k})|^2d\mathbf{k}, \quad (2.1)$$

where n and s denote filled and unfilled bands, respectively, $E_{ns}(\mathbf{k})=E_s(\mathbf{k})-E_n(\mathbf{k})$, and the interband oscillator strength is

$$M_{ns}{}^{j}(\mathbf{k})=\frac{1}{i}\int\psi_{\mathbf{k}n}{}^{*}\frac{\partial}{\partial x_j}\psi_{\mathbf{k}s}d\mathbf{r}. \quad (2.2)$$

In the crystal coordinate system the only nonzero tensor components are the diagonal components parallel ($\|$) and perpendicular ($\perp$) to the crystal c axis. Equation (2.1) neglects lifetime broadening effects such as phonon and impurity scattering.

The shape of the absorption spectra is essentially characterized by (1) the position of critical points in the band structure, i.e., points where $\nabla_{\mathbf{k}}E_{ns}(\mathbf{k})=0$ [thus the bands are parallel in this region, and a large contribution to $\epsilon_2(\omega)$ may result], and (2) the crystal symmetry selection rules which, along certain sym-

[11] A. H. Lettington, Ref. 9, p. 147.
[12] R. H. W. Graves and A. P. Lenham, J. Opt. Soc. Am. **58**, 126 (1968).
[13] E. F. W. Seymor and G. A. Styles, Phys. Letters **10**, 269 (1964); F. Borsa and R. G. Barnes, J. Phys. Chem. Solids **27**, 567 (1966); S. N. Sharma and D. L. Williams, Phys. Letters **25A**, 738 (1967).
[14] R. V. Kasowski (to be published).
[15] H. Ehrenreich and M. H. Cohen, Phys. Rev. **115**, 786 (1959).

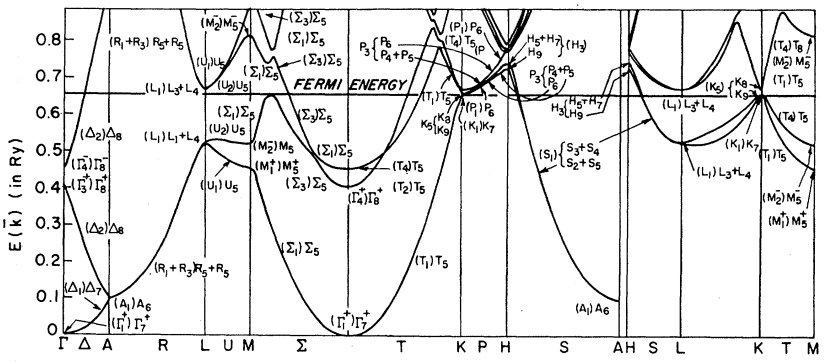

FIG. 1. Band structure of Zn at $T=0°$K.

metry directions, may require either $M_{ns}{}^{\parallel}$ or $M_{ns}{}^{\perp}$ to vanish (thus an anisotropy in the absorption results).

III. PSEUDOPOTENTIAL AND ENERGY BANDS FOR Zn AND Cd

We briefly discuss here a simple derivation of the PP formalism based on the orthogonality of the core and conduction-electron wave functions.[1]

The one-electron Schrödinger equation is

$$[T+V(\mathbf{r})]\psi_{\mathbf{k}}(\mathbf{r})=E_{\mathbf{k}}\psi_{\mathbf{k}}(\mathbf{r}), \tag{3.1}$$

where $V(\mathbf{r})$ is the self-consistent periodic potential of the ion cores, T is the kinetic-energy operator, $E_{\mathbf{k}}$ is the energy eigenvalue, and $\psi_{\mathbf{k}}$ is the one-electron wave function. The wave function $\psi_{\mathbf{k}}$ can be written as

$$\psi_{\mathbf{k}}(\mathbf{r})=\phi_{\mathbf{k}}(\mathbf{r})-\sum_{tj}|t,\mathbf{R}_j\rangle\langle t,\mathbf{R}_j|\phi_{\mathbf{k}}\rangle, \tag{3.2}$$

with

$$\phi_{\mathbf{k}}=\sum_{\mathbf{G}}\alpha_{\mathbf{G}+\mathbf{k}}|\mathbf{G}+\mathbf{k}\rangle, \tag{3.3}$$

where $|t,\mathbf{R}_j\rangle$ is a core state with quantum numbers t centered at the ion positions $\mathbf{R}_j$, and where $\mathbf{G}$ is a reciprocal-lattice vector; $|\mathbf{G}+\mathbf{k}\rangle$ denotes a normalized plane wave with wave vector $\mathbf{G}+\mathbf{k}$.

The one-electron wave equation (3.1), with the use of (3.2), can be rewritten as

$$(T+V+V_R)\phi_{\mathbf{k}}=E_{\mathbf{k}}\phi_{\mathbf{k}},$$

where

$$V_R\phi_{\mathbf{k}}=\sum(E_{\mathbf{k}}-E_t)|t,\mathbf{R}_j\rangle\langle t,\mathbf{R}_j|\phi_{\mathbf{k}}\rangle.$$

The operator V_R has the character of a repulsive potential which cancels out most of $V(\mathbf{r})$. Consequently, the electron can be thought of as moving in a smooth pseudopotential $V_{\text{eff}}=V+V_R$ with pseudo-wave-function $\phi_{\mathbf{k}}$.

The form of the empirical PP of SF is

$$V_{\text{eff}}=V_L+V_N+W_{\text{so}},$$

where V_L, V_N, and W_{so} are the local potential, the nonlocal potential, and the spin-orbit interaction, respectively. The components of V_{eff} have the following form:

(a) Local potential:

$$V_L(\mathbf{r})=\sum_{jh}V_L(\mathbf{G}_h)e^{i\mathbf{G}_h\cdot(\mathbf{r}-\mathbf{R}_j)},$$

where $V_L(G_h)$ has been fitted to experiment[2] and is taken to be nonzero for the {0002}, {10$\bar{1}$0}, {10$\bar{1}$1}, and {10$\bar{1}$2} reciprocal-lattice vectors in the hexagonal Brillouin zone; $\mathbf{R}_j$ labels the atomic sites.

(b) Nonlocal potential:

$$V_N=\sum_{tj}V(t)|t,\mathbf{R}_j\rangle\langle t,\mathbf{R}_j|,$$

where the index t runs over the s, p, and d states of the outermost occupied core shell. The functions $|t,\mathbf{R}_j\rangle$ are the Hartree-Foch-Slater atomic functions centered at the atomic sites $\mathbf{R}_j$, and the $V(t)$ are once again parameters determined by SF to fit experimental data.

(c) Spin-orbit term:

$$W_{\text{so}}(\mathbf{k},s,\mathbf{k}',s')=i[\lambda_p+\lambda_d(\mathbf{k}\cdot\mathbf{k}')]\mathbf{k}'\times\mathbf{k}\cdot\boldsymbol{\sigma}_{ss'},$$

where $\sigma_{ss'}$ are the s, s' components of the Pauli matrices.

The smooth pseudo-wave-function

$$\phi_{n\mathbf{k}}=\sum_{\mathbf{G}}\alpha_{\mathbf{G}+\mathbf{k}}{}^{n}|\mathbf{G}+\mathbf{k}\rangle$$

satisfies the pseudopotential wave equation

$$[(\mathbf{p}^2/2m)+V_L+V_N+W_{\text{so}}]\phi_{n\mathbf{k}}=E_{n\mathbf{k}}\phi_{n\mathbf{k}},$$

where n and $\mathbf{k}$ denote the band index and wave vector.

The PP parameters chosen by SF for Zn and Cd are given in Ref. 2, and the low-temperature band structures resulting from these parameters are displayed in Figs. 1 and 2, respectively. The band structures for Zn and Cd show similar departure from a free-electron hcp band structure in that the so-called butterflies[1] (third and fourth bands centered about L) are raised above the Fermi level. In Cd the monster (second-band-hole surface) is not connected across the ΓM symmetry line. These differences result from the large, nonlocal contribution to the PP from the outer d shells of the ion cores and affect the optical spectra significantly.

Spin-orbit coupling, on the other hand, is of much less importance, and it has not been included in the form of the PP used to calculate the optical properties

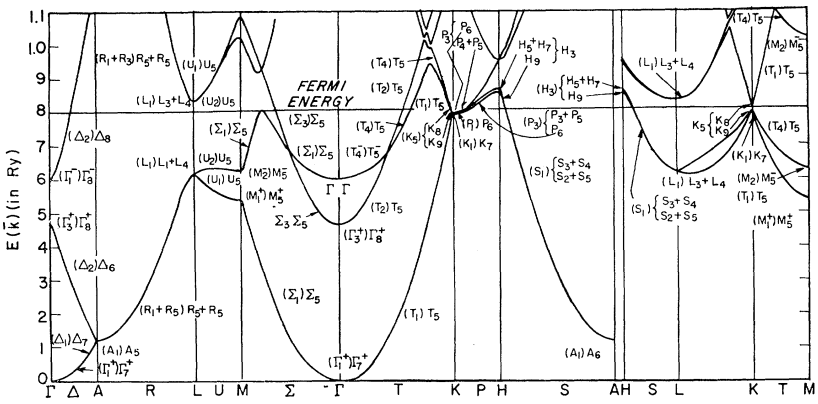

FIG. 2. Band structure of Cd at $T=0°K$.

here; i.e., we have made $\lambda_p=\lambda_d=0$. We have also calculated a band structure for Cd at $T=462°K$. This is done in a manner similar to that at $T=0°K$ except that the lattice parameters are slightly changed and the structure factor

$$S_0(\mathbf{G})=\cos 2\pi[\tfrac{1}{6}(h+2k)+\tfrac{1}{4}l]$$

is replaced by

$$S(\mathbf{G})=e^{-W(G,T)}S_0(\mathbf{G}).$$

Justification of this substitution, along with the value of $W(\mathbf{G},T)$ used, can be found in a previous paper by the author.[5]

The effect of the temperature smearing is to make the energy bands more free-electron-like. The butterflies drop below the Fermi surface, and the monster waist connects across the ΓM symmetry line.

Before performing the calculation of the optical spectra, we can qualitatively discuss which parts of the band structures give rise to the optical-absorption peaks. Figures 1 and 2 show that the second and third bands are nearly parallel along the ΓK, ΓM, and LH symmetry lines and thus contribute greatly to the absorption spectra. However, the energy difference between the second and third bands along LH are very sensitive to temperature: The third band (the butterfly) drops below the Fermi surface. Thus the contribution to the absorption from this region should be quite sensitive to the temperature. The interband energy separation along ΓK and ΓM is much less sensitive to temperature changes, and thus its contribution to the optical absorption undergoes far less change than that from the LH region.

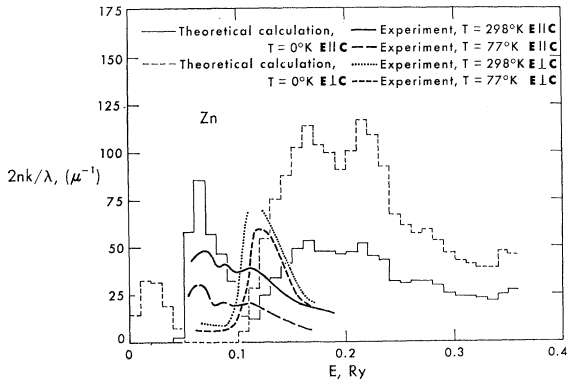

FIG. 3. Optical spectra of Zn at $T=0°K$.

IV. COMPUTATION OF IMAGINARY PART OF $\epsilon_2(\omega)$

In order to compute the dielectric function $\epsilon_2(\omega)$ numerically, we approximate it by a sum over a finite number of $\mathbf{k}$ points[16]:

$$\epsilon_2{}^j(\omega)=\frac{4\pi e^2\hbar^2}{m^2\omega^2}\frac{2}{(2\pi^2)}\frac{V_{BZ}}{\Delta\omega N}\times\sum_{ns}\sum_{\mathbf{k}}\delta^{\Delta\omega}(E_{ns}(\mathbf{k})-\hbar\omega)|M_{ns}{}^j(\mathbf{k})|^2, \quad (4.1)$$

where V_{BZ} is the volume of the Brillouin zone. $\delta^{\Delta\omega}(E_{n\,s}-\hbar\omega')$ is equal to unity if $|E_{n,s}-\hbar\omega'|<\frac{1}{2}\Delta\omega$ and is equal to zero otherwise. This will give a histogram for $\epsilon_2(\omega)$ in units of $\hbar\Delta\omega$. We have chosen $\hbar\Delta\omega=0.01$ Ry because the experimental optical spectra have only broad peaks and because of economical reasons. The oscillator strengths $M_{ns}{}^j(\mathbf{k})$ are calculated using the electron wave function $\psi_{\mathbf{k}}$, Eq. (3.2), which includes the core orthogonalized terms.

Equation (4.1) involves evaluation at many $\mathbf{k}$ points and consequently much computer time. We used here a sampling procedure whereby an exact calculation of the energy bands and interband oscillator strengths was performed for 197 $\mathbf{k}$ points. These $\mathbf{k}$ vectors are located on a mesh in a 1/24 symmetry section of the Brillouin zone such that the mesh points also serve as centers for 107 subzones. We then generated by a Monte Carlo method 15 029 $\mathbf{k}$ points in the above symmetry section. The corresponding eigenvalues and oscillator strengths at these points were obtained by quadratic interpolation according to the formula

$$f(\mathbf{k})=f(\mathbf{k}_0)+\sum_i(\mathbf{k}_i-\mathbf{k}_{0i})p_i+\sum_{ij}(\mathbf{k}_i-\mathbf{k}_{0i})q_{ij}(\mathbf{k}_j-k_{0j}), \quad (4.2)$$

[16] D. Brust, Phys. Rev. 134, 1337 (1964); R. Sandrock, *ibid.* 169, 642 (1968).

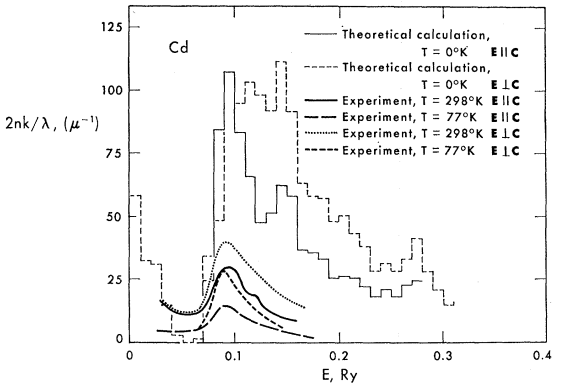

FIG. 4. Optical spectra of Cd at $T=0°K$.

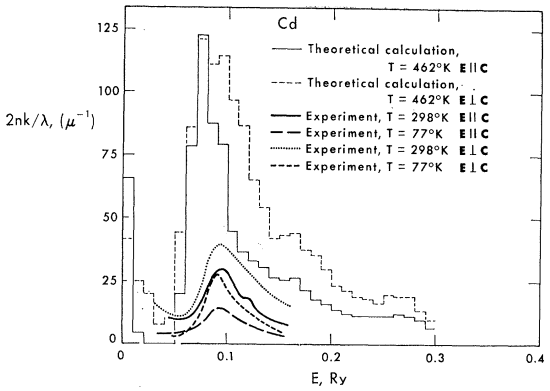

FIG. 5. Optical spectra of Cd at $T=462°K$.

where $\mathbf{k}_0$ is the subzone center in which the random point $\mathbf{k}$ falls, and $f(\mathbf{k})$ represents either an interband oscillator strength or an energy-band eigenvalue. The nine coefficients p_i, q_{ij} $(i \geq j)$ were determined by requiring (4.2) to be satisfied for the neighboring mesh points.

This numerical computation was performed for the $T=0°K$ band structures of Zn and Cd and for the $T=462°K$ band structure of Cd. The resultant curves for parallel and perpendicular polarization are represented in Figs. 3–5 along with the corresponding experimental data. The theoretical curves are represented as ϵ_2/λ in order to make comparison to experimental data more direct. Also, the experimental data are for $T=77$ and $T=298°K$. We should add once again that the broadening effects, which are important at high temperatures such as 462°K, are not included. However, we expect temperature effects to broaden the peaks somewhat symmetrically even for the $T=462°K$ result; under this assumption the calculated peak for 462°K is meaningful.

Several observations can be made about the theoretical and experimental curves:

(1) The calculated spectra at $T=0°K$ and $T=462°K$ exceed the magnitudes of the experimental spectra by as much as a factor of 4; in Al and Na the experimental values were greater than those of a theoretical calculation by a factor of 2.

(2) There is little agreement between experiment and the $T=0°K$ calculations except that, for parallel polarization, the main peaks fall at the same energies for both Cd and Zn.

(3) The $T=462°K$ calculated curves for Cd qualitatively agree with the 298°K experimental curves.

(4) The calculated spectra for Zn and Cd at $T=0°K$ are quite similar, as expected, because of the similarity in electronic structure.

Finally, in order to investigate the influence of the $\mathbf{k}$-dependent oscillator strength, the optical absorption for Cd at $T=0°K$ was calculated with a constant isotropic matrix element $|M_{ns}{}^j|=0.25$. The spectrum is given in Fig. 6 and is seen to be similar to that calculated in Fig. 4.

V. DISCUSSION AND COMPARISON WITH EXPERIMENT

The peaks in the optical absorption result from regions of the band structure where the energy bands are nearly parallel and the corresponding oscillator strengths are large. Such regions (see Figs. 1 and 2) occur along the symmetry lines ΓK, ΓM, and LH (the values of the oscillator strengths are discussed in detail in the latter part of this section). Along ΓK and ΓM, hcp symmetry selection rules allow direct electronic transitions from the second band to the third band ($T_4 \rightarrow T_2$ and $\Sigma_3 \rightarrow \Sigma_3$) only for parallel polarization light. Thus $M_{23}{}^{\perp}$ vanishes and this region contributes almost exclusively to the parallel polarization optical absorption. In the LH region, both oscillator strengths ($M^{\parallel}$ and $M^{\perp}$) are allowed for transitions from the degenerate first and second bands to the degenerate third and fourth bands ($S_1 \rightarrow S_1$). Thus this region contributes almost isotropically to the optical absorption.

The absorption spectra for perpendicular polarization is easy to explain since the peaks arise principally in the LH region. The Zn band structure in Fig. 1 shows that the allowed transitions begin at about 0.14 Ry

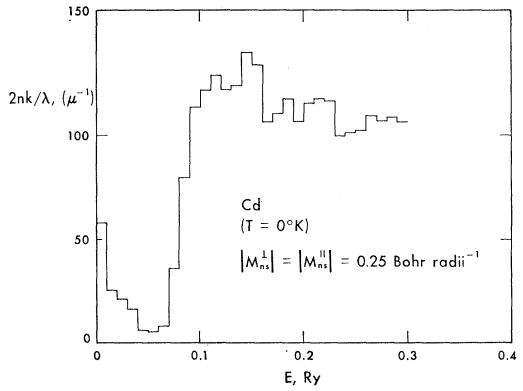

FIG. 6. Optical spectra of Cd at $T=0°K$ for a constant matrix element.

and extend to 0.24 Ry at the L point. The calculated peak in Fig. 3 has the same energy spread. Similarly, in Cd, the transitions begin at about 0.08 Ry and extend to about 0.15 Ry, which again gives rise to the calculated peak in Fig. 4.

At $T=0°$K the peak from the LH region appears to be a double peak. This is a result of the sharp change in slope (near the L point) in the second band. At this point the oscillator strengths are smaller than for the other points along the LH line. The double peak disappears if the third and fourth bands drop far enough below the Fermi surface at L.

From Figs. 3 and 4 we see that the agreement between theory ($T=0°$K) and experiment for perpendicular polarization is very poor since the peaks agree neither in position nor magnitude. However, the theoretical spectrum at $T=462°$K explains the reason for the disagreement in the positions of the peaks. The effect of temperature on the perpendicular spectrum is (1) to narrow the peaks, because the third and fourth bands at L drop below the Fermi surface, and (2) to shift the peaks to lower energy, because the crystal potential is smaller at high temperatures with a consequent reduction of the splitting between the second and third bands (which are degenerate in a free-electron model). These effects can be seen in the perpendicular spectrum for Cd ($T=462°$K) in Fig. 5. We see that the peak almost agrees with experiment, except that it has shifted slightly too much—past the experimental location. The position of the peak would have been much closer to the experimental peak had the calculation been performed at $T=298°$K.

The peaks in the parallel polarization spectra are explained just as simply. For Zn, the allowed transitions along ΓM and ΓK extend between 0.05 and 0.09 Ry, in excellent agreement with the calculated peak in Fig. 3. The secondary peak is a result of the LH region, and the explanation of it follows exactly that of the perpendicular polarization peak. The secondary peak is smaller than the corresponding peak for perpendicular polarization because along LH the $\perp$ oscillator strength is always larger than the $\parallel$ oscillator strength. The explanation is identical in Cd except that now the peaks overlap. The energy differences along ΓK and ΓM range 0.075–0.11 Ry, while along LH the energy difference ranges 0.075–0.15 Ry.

In contrast to the perpendicular case, there is some agreement between theory ($T=0°$K) and experiment in that the major peaks fall at the same energy. However, the secondary peaks (from the LH region) do not agree with experiment. This partial agreement indicates that the contribution from the ΓM, ΓK region is less sensitive to temperature than the LH region. This is in complete agreement with the characteristics of our temperature-dependent band structure that were pointed out in Sec. III. Figure 5 shows that the $T=462°$K calculated peak is overshifted with respect to the experimental peak at $T=298°$K.

Consequently, a qualitative understanding of the experimental spectra is gained by making use of the temperature-dependent PP that proved so successful in explaining the temperature dependence of the Knight shift in Cd.

The qualitative agreement in the shape and position of structure in the absorption spectra indicates that our band structure is reasonably good. The discrepancy in magnitudes between experiment and theory may, thus, be a result of the oscillator strength.

The electron wave function $\psi_{\mathbf{k}}$ of (3.2), not $\phi_{\mathbf{k}}$ of (3.3), was used to evaluate the oscillator strengths. At general points in the Brillouin zone, the oscillator strength is of the order of 0.08 Bohr radii^{-1}. Along the symmetry lines ΓM, ΓK, and LH, the oscillator strengths (for allowed transitions) are of the order of 0.50 Bohr radii^{-1}. In Al,[14] the average oscillator strength along symmetry lines was of the order of 0.22 Bohr radii^{-1}. One would roughly expect the optical absorption in Cd, then, to be roughly four times that of Al. A comparison of our calculated spectra with that calculated for Al [8] shows that in fact our Cd and Zn peaks are about four times larger than those of Al.

It is also instructive to compute the oscillator strengths using $\phi_{\mathbf{k}}$ of (3.3) in order to investigate the importance of the core contribution. In covalent crystals the core terms contribute only about 10% to $M_{ns}{}^{j}(\mathbf{k})$, and therefore $\phi_{\mathbf{k}}$ is generally used instead of $\psi_{\mathbf{k}}$. We find this a poor approximation for Zn and Cd at general points in the Brillouin zone: The core terms contribute as much as 50% to $M_{ns}{}^{j}(\mathbf{k})$. On the other hand, the approximation is excellent along the LH, ΓK, ΓM symmetry lines. There the bands are degenerate for zero crystal potential; for nonzero potential they are split into bonding and antibonding states. For these bonding-to-antibonding transitions, most of the oscillator strength lies in the region of interatomic overlap outside the atomic cores. As a result, the core terms contribute only about 10% to $M_{ns}{}^{j}(\mathbf{k})$. As in semiconductors, the same optical structure peaks then result whether we use $\psi_{\mathbf{k}}$ or $\phi_{\mathbf{k}}$; the background does depend on our using $\psi_{\mathbf{k}}$. The point to emphasize here is that the oscillator strengths for bonding-to-antibonding transitions should be comparable to those in semiconductors.

In conclusion, we wish to point out that the band structures of Zn and Cd as calculated by the PP method give a fairly good description of the optical spectra only if temperature-dependent effects are properly taken into account. More experiments at low temperatures would help to test these results further.

Note added in manuscript. More experimental work on Zn and Cd is under way using a different method, normal incidence reflectance.[17] Preliminary results show better agreement with the calculated spectra. The investigations are still incomplete, and definite state-

[17] G. Rubloff (private communication).

ments about comparison between experiment and theory cannot be made.

ACKNOWLEDGMENTS

It gives me pleasure to thank Professor L. M. Falicov for suggesting this problem and for his invaluable guidance and encouragement. This work has been directly supported by the National Science Foundation and the office of Naval Research. In addition, it has benefited from general support to the Material Sciences at the University of Chicago by the Advanced Research Projects Agency.

PHYSICAL REVIEW VOLUME 187, NUMBER 3 15 NOVEMBER 1969

Temperature-Dependent Knight Shift in Cadmium: A Theoretical Study

R. V. KASOWSKI*†

Department of Physics and James Franck Institute, The University of Chicago, Chicago, Illinois 60637

(Received 3 April 1969)

Experimentally the Knight shift in Cd is characterized by (1) an increase in the nuclear resonance frequency of more than 70% in the temperature range from 0 to 594°K (melting point), (2) an increase of 33% in the isotropic Knight shift at the melting point, and (3) an increase in the anisotropic Knight shift from a small negative value at $T=0$°K to a fairly large positive value at high temperatures. We find that this temperature dependence is theoretically accounted for by including the effects of lattice vibrations into the electronic structure which we have investigated by means of an empirical pseudopotential. The effect of the lattice vibrations is to decrease the strength of the pseudopotential. This makes the energy bands more free-electron-like, and the s character of the wave functions of the Fermi surface increases. It also destroys the cancellation of the contributions of the various p parts of the wave function to the anisotropic Knight shift, thus increasing the anisotropy as well. Many-body corrections were included by means of a temperature-independent enhancement factor and were determined empirically for $T=0$°K. The trend of the variation of the Knight shift with temperature, both isotropic and anisotropic, is explained.

I. INTRODUCTION

IN regard to its NMR properties, cadmium is not an ordinary metal. The variation of the resonance frequency with temperature T is more than eight times larger than that of any other metal.[1–4] Most metals exhibit a small fractional change in the isotropic Knight shift K_{iso} of generally less than 10% over the temperature range from 4°K to the melting point. In Cd, however, K_{iso} undergoes a fractional increase of about 70% in the temperature range from 4 to 594°K (melting point). Furthermore, upon melting, K_{iso} suffers an abrupt increase of 33%. Most metals show little change in K_{iso} at the melting point.

Cadmium is an hexagonal metal. Being noncubic, it exhibits an anisotropic Knight shift K_{an}.[5–7] The temperature dependence of K_{an} in Cd is also anomalous.[1–4] It starts from a small negative nonzero value at $T=0$°K, and after going through zero at a temperature between 0 and 60°K it increases to a fairly large value at the melting temperature.

The two results mentioned above seem to lead to a paradox. Since K_{iso} depends on the s part of the wave function, the first result seems to indicate that the wave function becomes more s-like as the temperature increases. The contribution to K_{an} depends mainly on the non-s character of the wave functions, mostly its p part. The fact that K_{an} increases with temperature would seem to indicate that the p character of the wave function also increases with temperature.

These temperature-dependent properties must somehow result from (1) the anisotropic expansion of the lattice with temperature and (2) the thermal lattice vibrations. Since the application of pressure to Cd does not reverse the large increase in either K_{iso} or K_{an},[8] the change in lattice parameters could not be a significant source of the anomalous temperature dependence.

The electronic properties of Cd at very low temperatures seems to be well accounted for. Stark and Falicov[9] (SF) have used de Haas–van Alphen (dHvA) data to fit an empirical nonlocal pseudopotential (PP). The Fermi surface resulting from this PP agrees to within a

* National Science Foundation Predoctoral Fellow. This work is being submitted as partial fulfillment for the requirements of the Ph.D. degree at the University of Chicago, Chicago, Ill.

† Present address: Central Research Dept. Experimental Station, E. I. DuPont de Nemours, Wilmington, Del.

[1] E. F. W. Seymor and G. A. Styles, Phys. Letters **10**, 269 (1964).

[2] F. Borsa and R. G. Barnes, J. Phys. Chem. Solids **27**, 567 (1966).

[3] S. N. Sharma and D. L. Williams, Phys. Letters **25A**, 738 (1967).

[4] R. G. Goodrich and S. A. Khan (to be published).

[5] A. Abragam, *The Principles of Nuclear Magnetism* (Oxford University Press, London, 1961).

[6] W. D. Knight, in *Solid State Physics*, edited by F. Seitz and D. Turnbull (Academic Press Inc., New York, 1956), Vol. II, p. 93.

[7] C. P. Slichter, *Principles of Magnetic Resonance* (Harper and Row Publishers, Inc., New York, 1963).

[8] T. Kushida and L. Rimai, Phys. Rev. **143**, 157 (1966).

[9] R. W. Stark and L. M. Falicov, Phys. Rev. Letters **19**, 795 (1967); and unpublished.